Morphological Transition of the Regular Structure of Poly(styrene-*block*-butadiene-*block*-styrene) at the Interface with Poly(xylenyl ether)

Mitsuteru Mutsuda*,† and Hitomi Omae‡

New Business Department, Daicel-Degussa Limited, 1-4-38, Minato-machi, Naniwa-ku, Osaka 556-0017, Japan, and Analysis Service Center, Daicel Chemical Industries, Limited, Himeji Research Park, 1239, Shinzaike, Hyogo 671-1283, Japan

Received August 8, 2003; Revised Manuscript Received December 18, 2003

ABSTRACT: It has been found that poly(styrene-*block*-butadiene-*block*-styrene) (SBS) forms a regular structure and the structure transforms into another regular structure at the interface with poly(xylenyl ether) (PXE). This study examines the order−order transition phenomena with a transition electron microscopy (TEM) and an atomic force microscopy (AFM). According to TEM observations, the thickness of the morphological transition area depends on a temperature and time. In some cases, the thickness of the new regular structure's area could reach 1000 nm. Such phenomena have not been reported yet. A layer of which viscoelasticity changes continuously is observed at the interface of PXE and SBS with an atomic force microscopy (AFM), and the thickness of the layer is almost same as the thickness of the morphology transition layer observed with TEM.

I. Introduction

Technologies controlling polymeric materials' morphology by making use of self-ordering properties of polymers are of great interest to academic researchers and now also to commercial developers. In particular, with reference to block copolymers, there has been a lot of work and investigation,[1] and it has been found that block copolymers composed of incompatible block segments generally form a microdomain structure in the solid state as a consequence of microphase separation of the constituent block chains in the solidification process.[2,3]

Regarding the transition of the morphology, three kinds of causes have been reported. The first one is the volume ratio of each segment of block copolymers. Hashimoto et al. have studied the relation between the morphology and the structure of block copolymers with a small-angle X-ray scattering (SAXS) and they have shown the mechanism of the self-ordering system thermodynamically.[4−7] It was also shown in the theoretical work, that the mechanism of a cylinder-lamellae transition in binary mixtures of diblock copolymers by Lyatskaya et al.[8] As for the combination of poly(*m*-xylenyl ether), (PXE) and poly(styrene-*block*-butadiene-*block*-styrene) triblock copolymer (SBS), it has been reported by Tucker et al., that the order structure of SBS changes to a disorder structure by blending PXE.[9] It was a order−disorder transition phenomenon in a homogeneous system.

The second one is the morphologies' forming conditions. The relationship between the morphology of poly(styrene-*block*-isoprene) diblock copolymers (SI), and their quenching conditions was reported by Winey et al.[10] Regarding the relationship between the morphology of SBS and its casting conditions such as the species of solvents, the annealing temperature, it was examined by Sakurai et al.[11] The order−disorder morphology transition of low molecular weight SI was investigated by Sakamoto et al., and they found two characteristic temperatures, i.e., the order−disorder transition temperature T_{ODT}, and the crossover temperature T_{MF} in the disordered state.[12]

The third one is a mechanical stress. For example, the effects of a shear deformation on the lamellae structure of polystyrene-*block*-poly(ethylene-*alt*-propylene) copolymer was reported by Okamoto et al.[13]

Although these previous works give us a lot of valuable information about morphologies of polymers, they mainly focused on a homogeneous system. In this study, it has been found that the order structure of SBS changes to another order structure at the heterogeneous interface of PXE and SBS; i.e., it is an order−order morphology transition phenomenon at a heterogeneous interface. The phenomena have not been reported yet.

The purpose of this study is to investigate the order−order transition of SBS at the heterogeneous interface with PXE, and to propose the mechanism.

II. Experimental Section

Materials. The materials' data are shown in Table 1. PXE-1, PXE-2, and SBS-1 were used in this study. The T_gs of each materials were determined from the first heat scanning of a differential scanning calorimeter (DSC) with molded specimens by the heat press process (for the heat press process, see the Methods section).

SBS triblock copolymer was prepared by a sequential living ionic polymerization. It could be assumed that the SBS had an symmetric structure, i.e., each polystyrene block was almost same length.[14] The microstructure of polybutadiene (PB) blocks was determined by infrared spectroscopy (Morero method[15]) to be 34, 55, and 11 mol % for *cis*-1,4-, *trans*-1,4-, and 1,2-linkages, respectively.

PXEs were synthesized by methods given in US Patents.[16,17] PXE-1 was a pure PXE and PXE-2 was a blend of 90 wt % PXE and 10 wt % of a high impact polystyrene (HIPS) by an extruder. The HIPS was prepared by a radical polymerization, and it contained 5.6 wt % of polybutadiene.

* Corresponding author.
† Daicel-Degussa Ltd. E-mail: m.mutsuda@daicel-degussa.com.
‡ Daicel Chemical Industries Ltd. E-mail: ht_omae@daicel.co.jp.

10.1021/ma035158t CCC: $27.50
Published on Web 04/03/2004

Table 1. Characteristics of Polymers in this Research[a]

polymer	M_n	M_w/M_n	other information	SBS-1	PXE-1	PXE-2
SBS	105 000	1.08	weight ratio of PS is 0.40	100		
PXE-A	17 200	2.76			100	
PXE-B	26 400	2.49				90
HIPS	85 700	2.13	weight ratio of PB is 0.056			10
T_g (°C) (determined by DSC)				−81.5 65.1	212.8	193.5

[a] The condition of DSC measurements was 20 °C/min

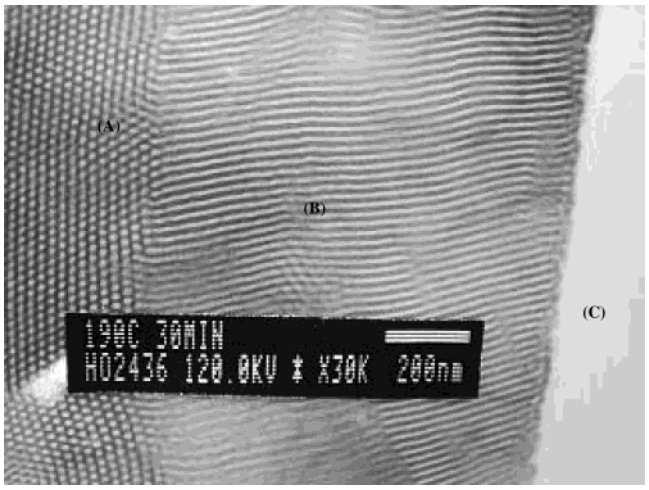

Figure 1. Example of TEM observations of the morphology at the interface of SBS-1 and PXE. This photo: combination of SBS-1 and PXE-1, heated at 190 °C for 30 min, under a pressure of 4.0×10^7 N/m^2 and after cooling to 25 °C for 3 min, under a pressure of 2.0×10^7 N/m^2.

Experimental Methods. SBS-1, PXE-1, and PXE-2 were molded into a square plate of 100 mm^2 and 1.0 mm thick by a heat press process. The conditions of the heat press process were as follows: 270 °C for 10 min, under a pressure of 4.0×10^7 N/m^2. After that, we cooled it down to 25 °C for 3 min, under a pressure of 2.0×10^7 N/m^2.

Adhesion specimens were prepared from these square plates. We put the plate of PXE-1 or PXE-2 on the plate of SBS-1, and set them into the square metal frame, 2 mm thick and 100 mm^2. They were sandwiched between two aluminum plates, the surfaces of which were finished by silicone polymer, and heated at a set temperature (the combination of SBS-1 and PXE-1, 190 °C; the combination of SBS-1 and PXE-2, 160 170, 175, 180, 185, 190 °C) for a set time (300−1800 s) under a pressure of 4.0×10^7 N/m^2. After that, the specimens were cooled to 25 °C for 3 min, under a pressure of 2.0×10^7 N/m^2.

Transmission electron microscopic (TEM) observations were performed with AJEM 1200EX II. From each dual layer, a section of about 160 nm thick was cut by a cryomicrotome Ultracut from Leica Ltd., with a diamond knife from Diatome AG. at −120 °C. The sections were mounted on cupper grids on which gold was evaporated. And the ultrathin sections were stained with osmium tetroxide (OsO_4) at a room temperature for 1 h. Only the butadiene segments of SBS were stained dark by OsO_4.

Atomic force microscopic (AFM) observations were performed at a room temperature with VE-AFM mode of SPI 3800HV from Seiko Instruments Information Devices Inc. using a sharp monocrystallized silicon DF-6 cantilever. To obtain a smooth surface for AFM observation, a dual layer was cut by a cryomicrotome Ultracut from Leica Ltd., with a diamond knife from Datome AG, at −120 °C.

III. Results and Discussion

The example of the typical morphology of SBS-1 at the interface with PXE-1 or PXE-2 is shown in Figure 1. We can see at least three distinct areas. These three areas are named as A, B, and C in order of their morphology and locations (Figure 1). A is the SBS's area and C is PXE's area because PXE is not stained by OsO_4. B is the morphology transition area, would be SBS or the mixture of SBS and PXE. All specimens in this study have these three distinct areas.

One of the most characteristic point in this phenomenon is that the morphology transition is an order−order transition. Figure 2 shows the morphologies of PXE-2 and SBS blend prepared by a casting with tetrahydrofuran, THF. By increasing the weight ratio of PXE-2, the morphology of the blend is changing from an order structure to an amorphous structure. It was the order−disorder transition. It is reasonable to suppose that this phenomenon was caused by the changing of the volume ratio of the butadiene segment and the styrene segment of SBS, because PXE is miscible to only the styrene segment of SBS.[4−6,9] Although we acknowledge that the species of solvents have an influence on morphologies,[11,18] this result suggests that the phenomenon at the heterogeneous interface is not the same as the phenomena at the homogeneous system.

Another characteristic point in this order−order transition phenomenon is that the morphology seems to change discontinuously between area(A) and area-(B). The observation planes of Figure 3, parts a and b, are orthogonal to each other. Comparing of area(A)s in Figure 3, parts a and b, it can be surmised that the morphology of area(A) is a cylinder structure such as hexagonal-packed cylindrical morphology. Parts a and b of Figure 4 show the interface between area(B) and area(C), i.e., the forefront of SBS. Though their observation planes are also orthogonal to each other, their

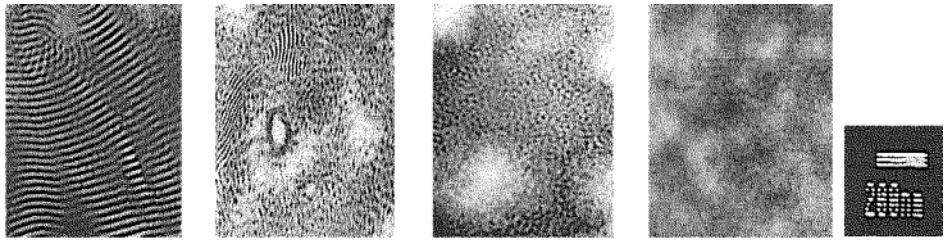

Figure 2. Morphologies of PXE-2 and SBS-1 blends prepared by casting with THF.

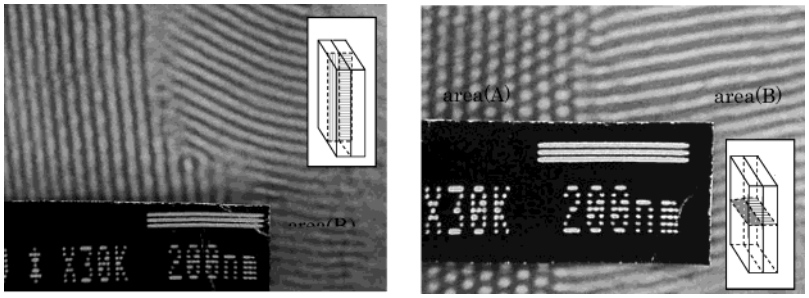

Figure 3. Observation of area(A) and area(B) by different observation planes. SBS-1 and PXE-1: heated at 190 °C for 30 min under a pressure of 4.0×10^7 N/m^2 and after being cooled down to 25 °C for 3 min under a pressure of 2.0×10^7 N/m^2.

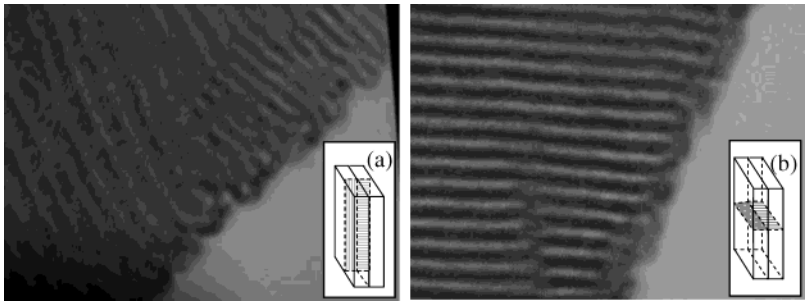

Figure 4. Observations of the forefront of SBS-1 by different observation planes. SBS-1 and PXE-1: heated at 190 °C for 30 min under a pressure of 4.0×10^7 N/m^2 and after being cooled down to 25 °C for 3 min under a pressure of 2.0×10^7 N/m^2.

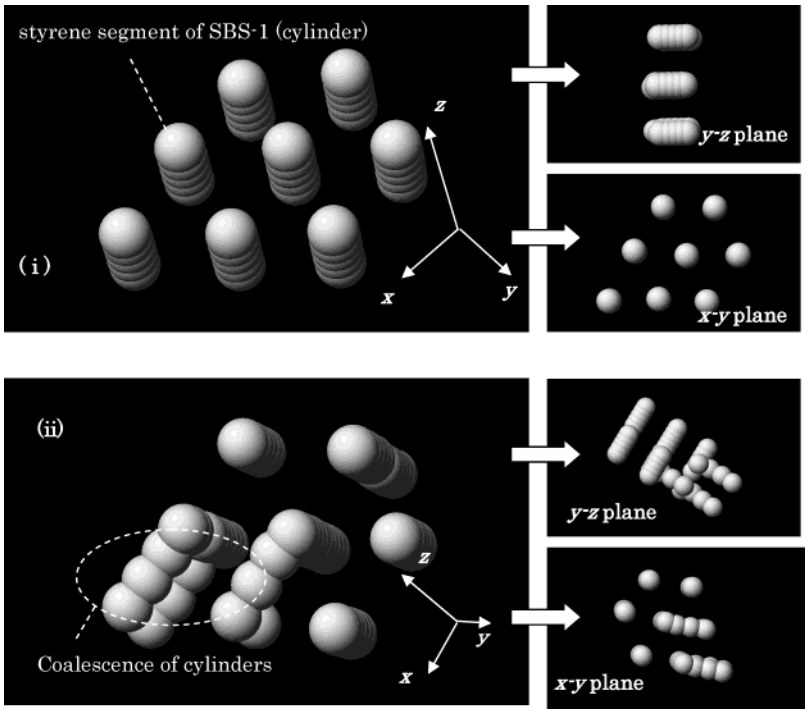

Figure 5. Hypothesis of the morphology of SBS-1 and its morphology transition.

morphologies look very similar to each other. This result suggests that the morphology of area(B) is a cylinder structure.

From these results, Figure 5 can be proposed as the morphology. Although it is difficult to determine the morphology by these TEM observations only, Figure 5 is consistent with the observation results. And it follows from the hypothesis of the morphology that a cylinder-cylinder coalescence can be proposed as the mechanism of the order−order morphology transition phenomenon. In this concept, (i) the morphology of SBS-1 would be the cylinder structure before the treatments with PXE-1 or PXE-2, and (ii) the cylinder coalescence would take place during the treatment process. This is the transition process without translational movement of the cylinders.

Regarding the cylinder−cylinder coalescence, it was also reported by Sakurai et al.[19] They reported about the morphology transition from cylindrical to lamellae microdomains of SBS on annealing at 150 °C. The scheme they proposed involved coalescence of cylinders, and precursory step to the cylinder coalescence would be the development of undulations along the length of the cylinders. The undulation would be primarily driven by a change in the interface curvature, i.e., the as-cast film would become unstable at the annealing temper-

Table 2. Correlations between the Thickness of the Area (*B*) and the Treatment Conditions[a]

	PXE-2						PXE-1
time (s)	160 °C	170 °C	175 °C	180 °C	185 °C	190 °C	190 °C
300		57 nm $\sigma = 32.2$		139 nm $\sigma = 14.1$	111 nm $\sigma = 19.6$	196 nm $\sigma = 104.3$	
600	48 nm $\sigma = 9.8$	145 nm $\sigma = 30.9$ 129 nm	159 nm $\sigma = 20.0$	247 nm $\sigma = 4.6$ 292 nm	254 nm $\sigma = 13.9$ 435 nm	222 nm $\sigma = 45.2$ 453 nm	650 nm
900		$\sigma = 29.4$		$\sigma = 19.3$	$\sigma = 99.8$	$\sigma = 123.2$	$\sigma = 113.6$
1200	60 nm $\sigma = 13.1$		294 nm $\sigma = 31.1$				
1500		441 nm $\sigma = 25.4$		314 nm $\sigma = 49.5$	598 nm $\sigma = 53.7$	699 nm $\sigma = 47.2$	
1800	130 nm $\sigma = 24.7$		480 nm $\sigma = 48.8$				1050 nm $\sigma = 111.6$

[a] σ: a standard deviation of each measurements

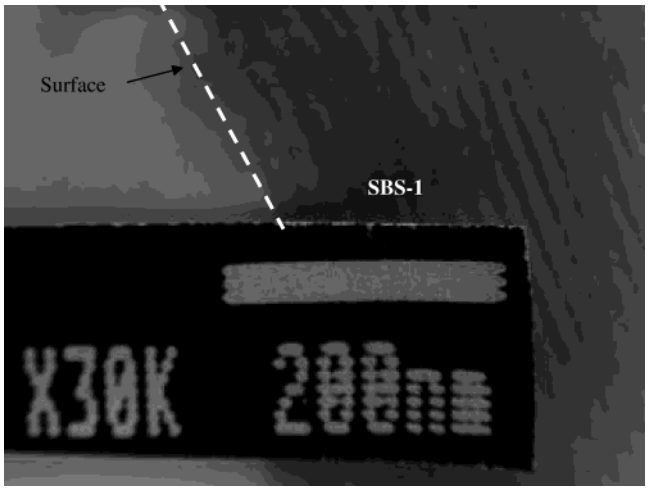

Figure 6. TEM observation of the morphology of SBS-1's surface without PXE: heat pressed at 180 °C for 30 min, under a pressure of 4.0×10^7 N/m^2 and after being cooled down to 25 °C for 3 min, under a pressure of 2.0×10^7 N/m^2.

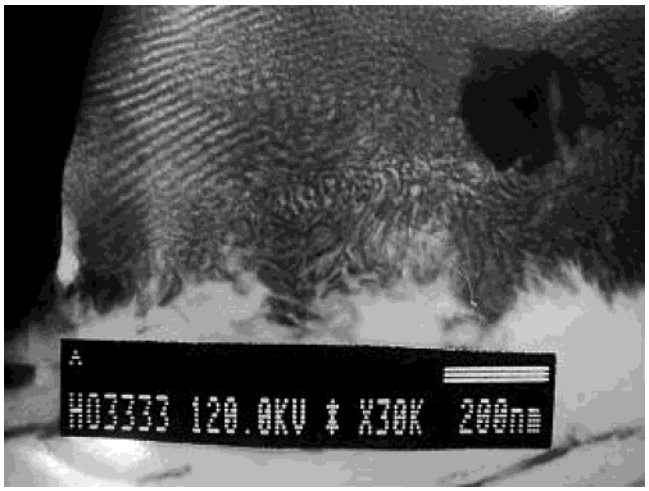

Figure 7. TEM observation of the interface of SBS-1 and PXE-2 without any mechanical pressure, treated at 180 °C for 30 min.

ature, and the systems would tend to achieve the new curvature equilibrium at the annealing temperature. Hence, it was proposed that the primarily physical factor associated with the process might be elastic deformation of the block chains and interfaces triggered by the relaxation of the unfavorable chain conformations for both polystyrene (PS) and polybutadiene (PB) blocks in the quasi-stable morphology frozen in the as-cast film.

Although we proposed this cylinders' coalescence concept as the mechanism of the order−order morphology transition, the driving force of the coalescence would be different from that of Sakurai's case. Figure 6 shows the morphology of SBS-1 without PXE, which is heat pressed at 180 °C for 30 min under a pressure of 4.0×10^7 N/m^2, and after cooled to 25 °C for 3 min under a pressure of 2.0×10^7 N/m^2. Any morphology transitions could not be observed. This result indicates that the morphology of SBS-1 is stable under the heat press process with PXE-1 or PXE-2. Figure 7 shows the morphology of the interface between SBS-1 and PXE-2 without any mechanical pressure. This specimen was treated at 180 °C for 30 min. Some morphology transition is observed in Figure 7. It follows from the results of Figures 6 and 7 that the shear stress[10] at the heat press process is not the main cause of the cylinder coalescence, even if the shear stress has some influence on the morphology transition phenomenon. It can be concluded that the morphology transition phenomenon is triggered by the existence of PXE. Therefore, on the assumption that the cylinder coalescence is the mechanism of the order−order transition phenomenon, we conclude that the cylinder coalescence is triggered by the existence of PXE.

The other characteristic point of this phenomenon is that the thickness of the morphology transition area depends on the treatment conditions such as time and temperature. Table 2 shows the thickness of the area-(B) in each heat press condition. Each thickness is determined by four TEM observations, the magnifications were 20 000× or 30 000×. In the case of 20 000× magnification, the field of vision of each picture was 2900 nm × 4075 nm of rectangular, and in the case of 30 000× magnification, the field of vision of each picture was 1930 nm × 2710 nm. Each picture has about a 2500−4000 nm length of the interface, and an average of 25 points of examination per picture was used as the thickness. Therefore, the thickness of each condition was determined by four pictures, i.e., it was determined by 100 analysis points per about 10 000−16 000 nm length of the interface. Parts a and b of Figure 8 and parts a and b of Figure 9 are the examples of the results. The dispersion of each data under each condition was about 10−20%.

The comparison between TEM observation and AFM observation is shown in Figure 10. About 850−1200 nm thickness for the morphology transition area is observed by TEM and about 1100 nm thickness for the layer of which the viscoelastic property is changing continuously

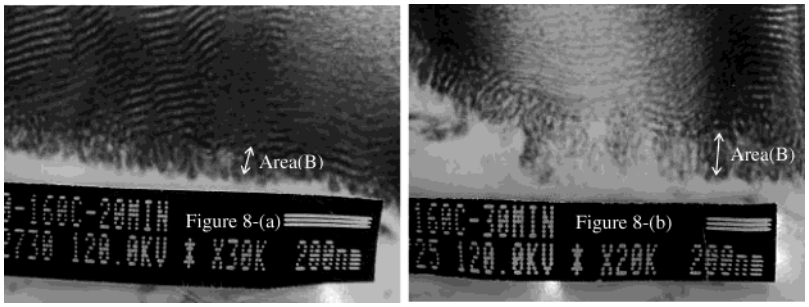

Figure 8. TEM observation of the interface of SBS-1 and PXE-2 at 160 °C for 30 min. The conditions are at 160 °C, under a pressure of 4.0×10^7 N/m^2 (a) for 20 and (b) for 30 min. After heating, it was cooled down to 25 °C for 3 min, under a pressure of 2.0×10^7 N/m^2.

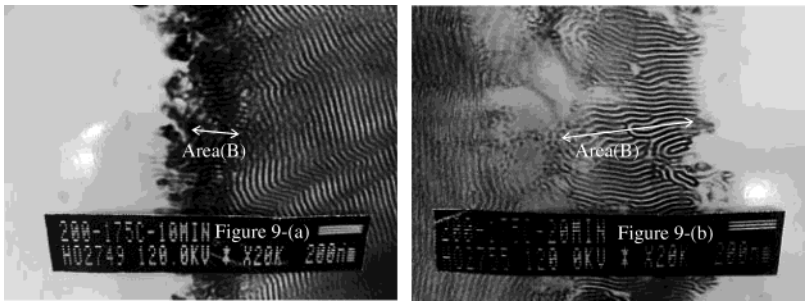

Figure 9. TEM observation of the interface of SBS-1 and PXE-2 at 175 °C. The condition are at 175 °C, under a pressure of 4.0 $\times 10^7$ N/m^2 (a) for 10 and (b) for 20 min. After heating, it was cooled down to 25 °C for 3 min, under a pressure of 2.0×10^7 N/m^2.

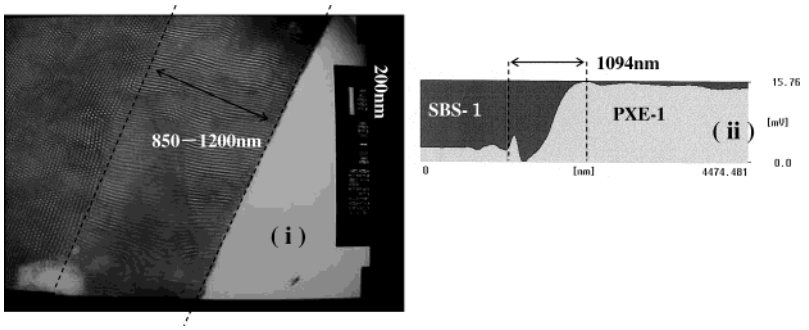

Figure 10. Comparison between TEM and AFM observation. The condition is; SBS-1 and PXE-1. The conditions are at 190 °C for 30 min under a pressure of 4.0×10^7 N/m^2, and after that it was cooled down to 25 °C for 3 min, under a pressure of 2.0×10^7 N/m^2. Key: (i) TEM observation, stained by OsO_4; (ii) AFM observation, with VE-AFM mode.

is observed by AFM between SBS-1 and PXE-1; i.e., the thickness of the layers which are observed by TEM and AFM, are almost the same order as each other. This fact suggests that the layer observed by AFM shows the information on the morphology transition area, area-(B), observed by TEM. This AFM observation result implies that component of materials would change at area(B). From these results and the temperature and the time dependencies of area(B)'s thickness (see Table 2, Figure 8, and Figure 9), it is reasonable to suppose that the morphology transition would be caused by an interdiffusion between PXE and SBS. Regarding the combination of PXE and PS, they are fully miscible due to the negative enthalpy of mixing[20,21] which is caused by the special interactions between the phenyl of PS and the phenylene or the methyl of PXE,[22−25] and the interdiffusion phenomena have been reported by, for example, Machate et al.,[21] and Composto et al.[26,27] The combinations of PXE-1 or PXE-2 and SBS-1 in this study are also fully miscible with each other, since their casting films from chloroform $CHCl_3$ are transparent and the changing of the T_g of the blends comformed to Flory−Huggins theory. Therefore, it may be presumed that PXE-1 or PXE-2 and SBS-1 diffuse each other and the interdiffusion phenomena cause the order−order morphology transition. On this assumption, we calculated the interdiffusion coefficients D and the activation energy of the diffusion based on the previous reports[21,26,27] and examined their validity as follows.

In the case of an interdiffusion between two kinds of polymers, e.g., polymer A and polymer B, using Flory−Huggins theory, D can be written as[21,28]

$$D = 2(\chi_s - \chi)\phi_A\phi_B D_T \tag{1}$$

where χ is the Flory segment−segment interaction parameter, χ_s is the Flory segment−segment parameter at the spinodal, and φ_A, φ_B are the volume fractions of polymers A and B, and D_T is an Onsager transport coefficient. When these two polymers are different, i.e., when their mobilities are different, the following two theories are proposed for analyzing a polymer−polymer interdiffusion phenomena.

The "slow theory"[28,29] requires that the fluxes of the polymers can be canceled. Therefore,

$$D_T^{-1} = \phi_B(D_A^* N_A)^{-1} + \phi_A(D_B^* N_B)^{-1} \tag{2}$$

where N_A and N_B are the degrees of polymerization of polymers A and B, respectively, and D_A^* and D_B^* are the tracer diffusion coefficients of each polymer. From the standpoint of "slow theory", the diffusion of the faster moving component is slowed by the other. Therefore, the "slow theory" predicts that the slower moving component controls D; i.e., D is practically independent of the molecular weight of the fast component.

The "fast theory"[30,31] requires that osmotic pressure gradients can be canceled. Therefore,

$$D_T = \phi_B D_A^* N_A + \phi_A D_B^* N_B \quad (3)$$

From the standpoint of the "fast theory", if one component diffuses much faster than the other, for example $D_A^* \gg D_B^*$, the faster moving component, in this case polymer *A*, controls D; i.e., the "fast theory" predicted that D is inversely proportional to the molecular weight of the fast component.

Composto et al. examined the polymer−polymer interdiffusion phenomena between PXE and PS above the T_g of PXE.[26,27] According to them, the molecular weight dependent on D_{PS}^* in a pure PXE matrix was shown to conform to the reputation model. D_{PS}^* was in the range 10^{-13}−10^{-12} cm^2 s^{-2}, and it was 2 orders of magnitude higher than D_{PXE}^*. And they concluded that the interdiffusion phenomena could be explained with "fast theory". Machate et al. also reported about the interdiffusion phenomena between PXE and PS, and their results also suggest that the phenomena are conformed to "fast theory".[21]

In this study, our heat press temperatures are much higher than the T_g of SBS-1 and are a little lower than the T_g of PXE-1 and PXE-2 (see Table 1). Therefore, it is reasonable to suppose that these combinations in this study also conform to "fast theory" if the phenomena is caused by the interdiffusion. When Fick's second law applies,[21] as written in the following eq 4, where only SBS-1 molecules diffuse based on "fast theory"

$$\frac{\partial C}{\partial t} = D\frac{\partial^2 C}{\partial x^2} \quad (4)$$

where C denotes the SBS-1 concentration at coordinate x. Assuming a semi-infinite medium, where the PXE layer is thicker than the interdiffusion zone (i.e., the SBS-1 concentration varies from 0 to 100%), the initial condition is

$$t = 0; \quad C = 0 \quad (5)$$

and the boundary condition is

$$x = \infty; \quad C = 0 \quad (6)$$

Finally eq 7 was obtained.

$$C = -C_0 \,\mathrm{erf}(\zeta) + C_0$$

$$\therefore \frac{C}{C_0} = 1 - \mathrm{erf}(\zeta) = \mathrm{erfc}(\zeta) = \mathrm{erfc}\left(\frac{x}{2\sqrt{D_A t}}\right) \quad (7)$$

where C is the concentration at the phase boundary of the interface of SBS-1 and PXE-1 or PXE-2, and C_0 is the concentration at the boundary of the morphology transition, in the case of this experiment. The tables of the correlation between a and b in $b = erf(a)$ have already been published,[32] and here C/C_0 is a constant; therefore eq 7 shows that x, i.e., the thickness of the area(B) should be in direct proportion to the square root of the treatment time, $t^{1/2}$. When we assumed that C is almost zero and C_0 equals 1.0, from eq 7

$$\mathrm{erfc}\left(\frac{x}{2\sqrt{D_{PXE-1} \cdot t}}\right) = \frac{C}{C_0} \doteqdot \frac{0}{1} = 0$$

$$\therefore \frac{x}{2\sqrt{D_{PXE-1} t}} \doteqdot 3.0$$

$$\therefore x = 6\sqrt{D_{PXE-1}} \times \sqrt{t} \quad (8)$$

In Figure 11, the thickness of the area(B) is plotted against the square root of the treatment time $t^{1/2}$. The first-order approximate curves of each plot and calculated each interdiffusion coefficient D are shown in Table 3. Figure 12 shows an Arrhenius plot for D of PXE-2, and from the result, we obtained

$$D = \mathrm{A}\exp(-E_a/RT) = 9.5 \times 10^4 \exp(-86.5/RT) \quad (9)$$

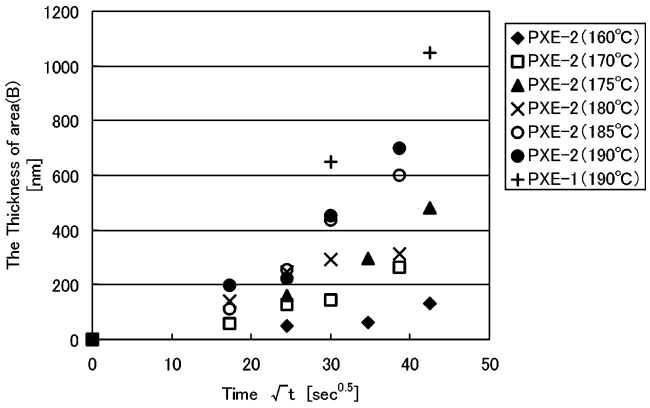

Figure 11. Thickness of the area (*B*) vs square root of time ($s^{0.5}$).

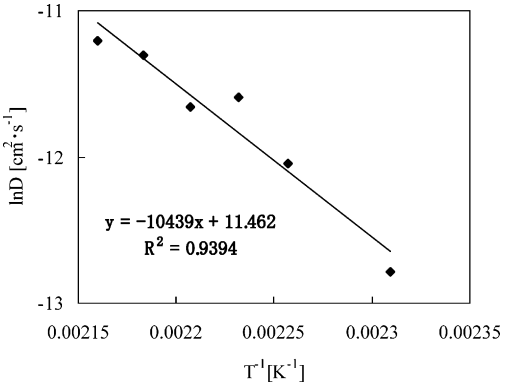

Figure 12. Arrhenius plot for D of PXE-2 in Table 3.

Table 3. First-Order Approximate Curves and the Interdiffusion Coefficient *D*

		first-order approximate curves x (nm) = $at^{0.5}$ ($s^{0.5}$)		
PXE	temp (°C)	a	correlation coeff R^2	D (cm^2·s^{-1})
PXE-1	190	23.7	0.99	1.56×10^{-11}
PXE-2	190	15.0	0.86	6.25×10^{-12}
	185	13.4	0.88	4.99×10^{-12}
	180	8.90	0.96	2.20×10^{-12}
	175	9.57	0.90	2.54×10^{-12}
	170	5.69	0.89	8.99×10^{-13}
	160	2.44	0.83	1.65×10^{-13}

where R is the gas constant, T is the temperature for the diffusion (K). The eq 9 shows the activation energy E_a of the interdiffusion between SBS-1 and PXE-2 as 86.5 kJ/mol. According to the previous work by Machate et al.,[21] the activation energy of the diffusion of PXE ($M_w = 39\ 100$) and PS ($M_w = 100\ 000$) combination was 104 kJ/mol, and the D of this combination was 5.6×10^{-12} cm^2/s at 200 °C. From the result, the D at 190 °C can be estimated as about 3×10^{-12}–4×10^{-12} cm^2/s. Compared with our experimental results and the previous work, no large inconsistency could be found between them.

Machate et al. tried to examine also about the interdiffusion phenomena between PXE and poly(styrene-*block*-butadiene) (SB) by TEM observations of the morphology transition of SB, however they could not observe any morphology transitions of the SB even at a higher temperature than our experiments.[33] They concluded that the diffusion zones of the PXE and the SB were limited in thickness by the incompatibility of the PXE and the butadiene segment of the SB. However, the SB's weight-average molecular weight was 130 000 and the styrene content was 59 wt %; i.e., the volume ratio of the styrene segment of the SB was bigger than that of SBS-1, and that of the butadiene segment of the SB was smaller than that of SBS-1. Therefore, it is difficult to suppose that the PXE and the SB could not diffuse each other because of the incompatibility of the PXE and the butadiene segment of the SB. In light of our experimental results, it would be rather reasonable to hypothesize that the PXE and the SB diffused with each other without any morphology transitions in their experiments.

IV. Conclusion

Order−order transition of the morphology of SBS at the interface with PXE has been observed with TEM, and the transition depends on the treatment time and temperature. One of the important points to emphasize is that the growth of the morphological transition at the heterogeneous interface has not been observed yet. In some cases, the depth of the transition area reached around 1000 nm. We have surmised the cause by a process of elimination, which was deformation and coalescence of the polystyrene's cylinders of SBS triggered by the existence of PXE.

This phenomenon still has some inexplainable points. For example, previous works indicated that the main diffusion was caused by the diffusion of polystyrene copolymer, in the case of the interdiffusion between polystyrene copolymer and PXE.[21,26,27] If these previous results can be applied to our experimental results, we must conclude that SBS-1 diffuses into PXE-1 or PXE-2 keeping its order structure before the cylinder coalescence causes, however it cannot reasonably be assumed. On the other hand, it also cannot reasonably be assumed that the main diffusion would be caused by the diffusion of PXE compared with the T_g of PXE and SBS.

The future direction of this study will be one that analyzes the morphology in more detail with SAX, TEM, and some kind of three-dimensional observation[37] etc. as well as examining other material combinations.

It follows from these results that surface condition has a great influence on the morphology not only at the interface but also deep inside of the materials. We expect that it will open up numerous possibilities in the technology of control of polymeric materials' morphology.

References and Notes

(1) See, for example: Matsuo, M.; Ueno, T.; Horino, H.; Chujyo, S.; Asai, H. *Polymer* **1968**, *9*, 425.
(2) Molau, G. E. *Block Polymers*; Aggarwal, S. L.; Ed.; Plenum Press: New York, 1970; p 79.
(3) Inoue, T.; Soen, T.; Hashimoto, T.; Kawai, H. *J. Polym. Sci., Part A-2*, **1969**, *7*, 1283.
(4) Hashimoto, T.; Shibayama, M.; Kawai, H. *Macromolecules* **1980**, *13*, 1237.
(5) Hashimoto, T.; Shibayama, M.; Kawai, H. *Macromolecules* **1983**, *16*, 1093.
(6) Ehlich, D.; Takenaka, M.; Hashimoto, T. *Macromolecules* **1993**, *26*, 492.
(7) Tanaka, H.; Hasegawa, H.; Yamasaki, K.; Hashimoto, T. *Macromolecules* **1987**, *20*, 1651.
(8) Ju. Lyatskaya, V.; Zhulina, E. B.; Birshtein, T. M. *Polymer* **1992**, *33*, 343.
(9) Tucker, P. S.; Barlow, J. W.; Paul, D. R. *Macromolecules* **1988**, *21*, 1678.
(10) Winey, K. I.; Patel, S. S.; Larson, R. G.; Watanabe, H. *Macromolecules* **1993**, *26*, 4373.
(11) Sakurai, S.; Momii, T.; Taie, K.; Shibayama, M.; Nomura, S.; Hashimoto, T. *Macromolecules* **1993**, *26*, 485.
(12) Sakamoto, N.; Hashimoto, T. *Macromolecules* **1995**, *28*, 6825.
(13) Okamoto, S.; Saijo, K.; Hashimoto, T. *Macromolecules* **1994**, *27*, 5547.
(14) Shultz, A. R.; Beach, B. M. *J. Appl. Polym. Sci.* **1977**, *21*, 2305.
(15) Morero, D.; Santambrigio, A.; Pori, L.; Ciampelli, E. *Chem. Ind.* (*Milan*), **1959**, *41*, 758.
(16) Hay, A. S. (General Electric) US 3306874 1962; *Chem. Abstr.* **1965**, *62*, 2846.
(17) Hay, A. S. (General Electric) US 3306875 1962; *Chem. Abstr.* **1965**, *62*, 708.
(18) Hasegawa, H.; Tanaka, H.; Yamasaki, K.; Hashimoto, T. *Macromolecules* **1987**, *20*, 1651.
(19) Sakurai, S.; Momii, T.; Taie, K.; Shibayama, M.; Nomura, S.; Hashimoto, T. *Macromolecules* **1993**, *26*, 485.
(20) Fried, J. R. In *Developments in Polymer Characterization-4*; Dawkins, J. V., Ed.; Applied Science Publishers: London, New York, 1983.
(21) Machate, C.; Lohmar, J.; Dröscher, M. *Macromol. Chem.* **1990**, *191*, 3011.
(22) Li, S.; Rice, D. M.; Karaz, F. E. *Macromolecules* **1994**, *27*, 2211.
(23) Feng, H.; Feng, Z.; Ruan, H.; Shen, L. *Macromolecules* **1992**, *25*, 5981.
(24) Wang, P.; Jones, A. A.; Inglefield, P. T.; White, D. M.; Bendler, J. T. *New Polym. Mater.* **1990**, *2* (3), 221.
(25) Wellinghoff, S. T.; Koening, J. L.; Baser, E. *J. Polym. Sci.* **1977**, *15*, 1913.
(26) Composto, R. J.; Kramer, E. J.; White, D. M. *Nature* **1987**, *328*, 234.
(27) Composto, R. J.; Kramer, E. J.; White, D. M. *Macromolecules* **1988**, *21*, 2580.
(28) Brochard, F.; Jouffroy, J.; Levinson, P. *Macromolecules* **1983**, *16*, 1638.
(29) Binder, K.; *J. Chem. Phys.* **1983**, *79*, 6387.
(30) Kramer, E. J.; Green, P.; Palstrom, C. J. *Polymer* **1984**, *25*, 473.
(31) Sillescu, H. *Macromol. Chem. rapid Commun.* **1984**, *5*, 519.
(32) See, for example: Crank, J. *The Mathematics of Diffusion*, 2nd ed.; Oxford University Press: New York, 1975.
(33) Machate, C.; Lohmar, J.; Dröscher, M. *Macromol. Chem.* **1990**, *191*, 3026.
(34) Jinnai, H.; Nishikawa, Y.; Koga, T.; Hashimoto, T. *Macromolecules* **1995**, *28*, 4782.

MA035158T